



Stable cluster of identical water droplets formed under the infrared irradiation: Experimental study and theoretical modeling

Leonid A. Dombrovsky^{a,b,*}, Alexander A. Fedorets^b, Vladimir Yu Levashov^c,
Alexei P. Kryukov^d, Edward Bormashenko^e, Michael Nosonovsky^{b,f}

^aJoint Institute for High Temperatures, 17A Krasnokazarmennaya St, Moscow 111116, Russian Federation

^bX-BIO Institute, University of Tyumen, 6 Volodarskogo St, Tyumen 625003, Russian Federation

^cInstitute of Mechanics of Moscow State University, 1 Michurinskiy Prosp., Moscow 119192, Russian Federation

^dMoscow Power Engineering Institute, 14 Krasnokazarmennaya St, Moscow 111250, Russian Federation

^eDepartment of Chemical Engineering, Biotechnology and Materials, Ariel University, Ariel 40700, Israel

^fDepartment of Mechanical Engineering, University of Wisconsin–Milwaukee, 3200 North Cramer St, Milwaukee, WI 53211, United States

ARTICLE INFO

Article history:

Received 18 May 2020

Revised 21 July 2020

Accepted 24 July 2020

Keywords:

Droplet cluster
Evaporation
Condensation
Infrared radiation
Stability
Modeling

ABSTRACT

Infrared irradiation of a droplet cluster has been used during several years as the main method of preventing coalescence of the cluster with a layer of water. The desired effect is achieved by suppressing the condensational growth of large droplets. In new experiments, it was first discovered that prolonged exposure to infrared radiation leads to asymptotic equalization of radii of various droplets. A theoretical analysis of the experimental results was carried out on the basis of the developed model for transient heat transfer. The suggested model includes the thermal effect of infrared radiation, the dynamics of the combined process of evaporation and condensation, as well as convective heat transfer with the surrounding humid air. When calculating the infrared heating of semi-transparent water droplets, the spectral composition of the external radiation is taken into account. The evaporation and condensation of water droplets is considered taking into account the kinetics of the process in the Knudsen layer and the vapor diffusion in the outer part of the boundary layer. Simple analytical relations are obtained for the asymptotic equilibrium parameters of small droplets. The numerical data for the time variation in the size of cluster droplets streamlined by a mixture of air and supersaturated water vapor are in good agreement with the results of laboratory measurements.

© 2020 Elsevier Ltd. All rights reserved.

1. Introduction

The natural behavior of droplet clusters levitating in an ascending vapor-air flow over the locally heated water surface is characterized by a fast growing of droplets due to the condensation of water vapor and the final coalescence of large droplets with the lower layer of water [1–4]. The suppression of the condensational growth of water droplets of a cluster with the use of infrared irradiation of droplets was observed for the first time in [5,6] and considered also by the authors in paper [7]. It was shown that the required power of infrared radiation is only 6% of the power of laser used for heating of water layer. The authors' intention to use the droplets of a cluster as unique biochemical microreactors [8,9] was a motivation for studying long-term infrared irradiation on cluster behavior. The observed alignment of sizes of various droplets and

the dependence of the resulting equilibrium radius of droplets on the water layer temperature and irradiation intensity are the subjects of the paper.

The objective of the paper is two-fold: (1) to determine experimentally the thermal conditions under which prolonged exposure to infrared radiation on a levitating droplet cluster leads to the formation of an equilibrium cluster of identical water droplets, (2) to develop a theoretical model for both the parameters of the equilibrium cluster and the process of the asymptotic transition of the cluster to the equilibrium state. Of course, the calculated variations of the radii of single water droplets over time should be compared with the results of laboratory measurements.

2. Laboratory set-up and experimental procedure

The schematic of the experiments performed at the Microdynamic Technologies Laboratory of the University of Tyumen is presented in Fig. 1. The thermostatically controlled cuvette of water at 15 °C made it possible to stabilize the temperature regime in the

* Corresponding author.

E-mail address: ldomb@yandex.ru (L.A. Dombrovsky).

Nomenclature

a	radius of droplet
b	radius of cluster
c	specific heat capacity
D	diffusion coefficient
Fo	Fourier number
f	coefficient in Eq. (4)
h	convective heat transfer coefficient
k	thermal conductivity
L	latent heat of evaporation
l	mean free path of molecules
M	molecular mass
\dot{m}	mass flow rate of evaporation
Nu	Nusselt number
P	absorbed radiation power
p	pressure
Q	efficiency factor
q	radiative flux
R	gas constant
T	temperature
t	time
x	diffraction parameter

Greek symbols

α	thermal diffusivity
γ	coefficient in Eq. (12)
λ	wavelength
ρ	density
τ	characteristic time
ϕ	relative humidity
ψ	function introduced by Eq. (4)

Subscripts and superscripts

a	absorption
air	air
gas	gas
ev	evaporation
eq	equilibrium
K	Knudsen
mol	molecular
rel	relaxation
s	surface
sat	saturation
th	thermal
vap	vapor
w	water
λ	spectral
0	initial or reference value

cluster generation region. The water layer thickness of $400 \pm 1 \mu\text{m}$ was monitored by an IFC2451 laser confocal sensor (Micro-Epsilon, USA). The local heating region was induced by a BrixX 808–800HP laser beam of diameter about 1 mm (Omicron Laserage, Germany) with the wavelength of $0.808 \mu\text{m}$ and maximum power of 800 mW).

Two miniature emitters of infrared radiation EK-8520 (Helioworks, USA) were used. At the level of the water surface, the beam diameter of these emitters exceeded 10 mm. As a result, the droplets and the underlying water layer were subjected to almost uniform irradiation (the emission spectrum is presented in [6]). Infrared emitters were located symmetrically on two opposite sides and were oriented at an angle of 45° (Fig. 1). The temperature of water surface under the cluster was monitored by an LT-CF2–C3 pyrometric sensor (Micro-Epsilon, USA; wavelength range from 8

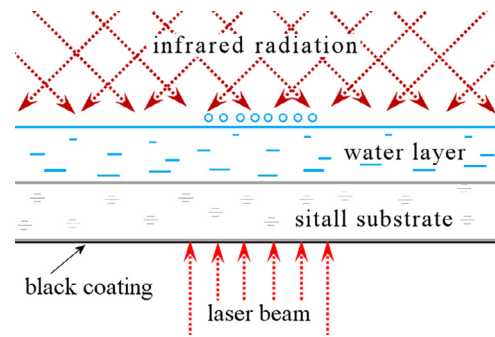


Fig. 1. The schematic of local laser heating of water and infrared irradiation of levitating droplets. The droplet cluster is shown as several small blue circles just above the water layer. (For interpretation of the references to colour in this figure legend, the reader is referred to the web version of this article.)

to $14 \mu\text{m}$). AXIO Zoom. The V16 stereo microscope (Zeiss, Germany) equipped with an EDGE 5.5C camera (PCO, Germany) was used for video recording. The experiments were carried out with distilled water containing natural impurities of surfactants, which provided suppression of thermocapillary flows.

3. Experimental results

In the case of insufficiently high infrared radiative flux, the cluster droplets continue to grow due to the condensation of water vapor, and this process will end with coalescence of large droplets with a layer of water. Obviously, at a certain minimum radiative flux, a transition to gradual stabilization of a cluster consisting of droplets of various sizes should be observed. In this case, larger droplets can decrease in size, and smaller droplets increase. With prolonged exposure to infrared radiation, equalization of droplets radii in the cluster and an asymptotic transition to an equilibrium cluster of identical droplets are expected.

For clarity, from a series of laboratory experiments, we selected for the present paper the results obtained for a small cluster consisting of six droplets, the sizes of which initially differ significantly from each other. The photographs in Fig. 2 taken at various stages of the process illustrate the transition to an equilibrium cluster. The measured current radii of all six droplets are presented in Fig. 3. The stepwise nature of the curves is a result of the limited spatial resolution of digital images with a pixel size of about $0.6 \mu\text{m}$. One can see that infrared irradiation leads to a decrease in the radius of droplets 1 and 2 and an increase in the radius of droplets 4, 5, and 6. The radius of droplet 3 remains constant and equal to the equilibrium value.

It is convenient to characterize the heating of the water surface under the cluster with the temperature without infrared irradiation, T_{s0} , (the laser heating only) and also with the increase in this temperature, $\Delta T_s = T_s - T_{s0}$, due to absorption of the infrared radiation. Experiments at different intensities of infrared radiation showed that there is a boundary separating the region, in which the condensational growth only slows down (but there is a coalescence with the water layer), from the region where the asymptotic stabilization of clusters is observed. One can see in Fig. 4a that this boundary is in the narrow range of $6 < \Delta T_s/T_{s0} < 9\%$. As one can expect, the minimum equilibrium radius of water droplets, a_{eq} , at this boundary decreases monotonically with the increasing intensity of infrared irradiation. This is illustrated in Fig. 4b, where the dots show the results of a series of laboratory experiments. Note that the ratio $\Delta T_s/T_{s0}$ shown on the abscissa in Fig. 4b is proportional to the infrared radiative flux.

For better understanding the results presented in Fig. 4a, it should be noted that one can obtain different values of the equi-

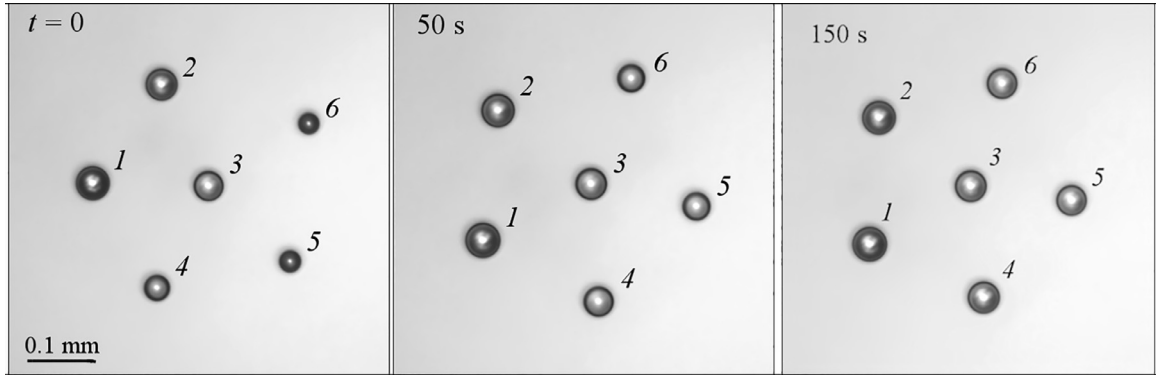


Fig. 2. The evolution of droplet cluster during the long-term infrared irradiation.

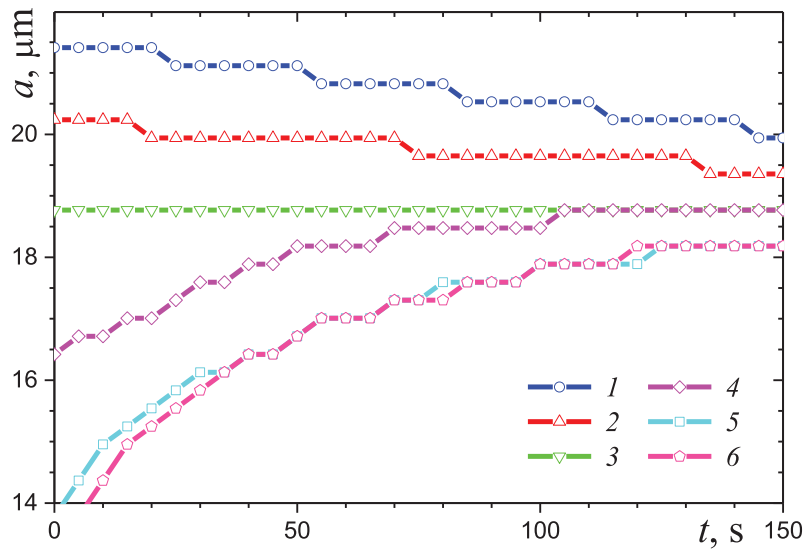


Fig. 3. Time variation of radius of water droplets with numbers from 1 to 6 (see Fig. 2). The stepwise nature of the curves is a result of a purely high resolution of digital image with a pixel size of about 0.6 μm .

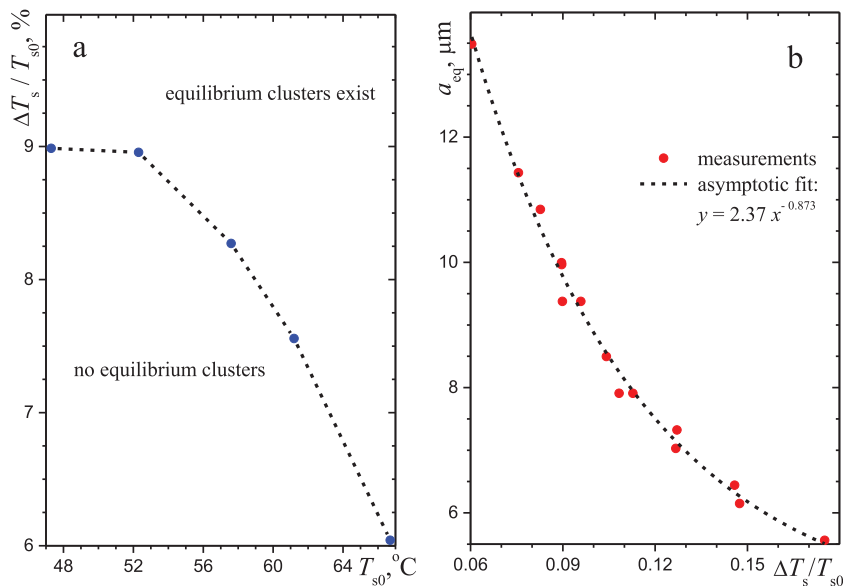


Fig. 4. The equilibrium of irradiated droplet clusters: a – the region of possible equilibrium clusters, b – the equilibrium radius of levitating water droplets. The value of T_{s0} is measured in $^{\circ}\text{C}$.

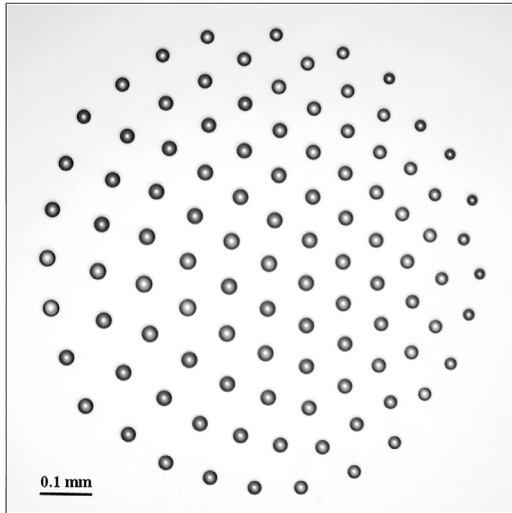


Fig. 5. A typical upper view of the droplet cluster consisting of a large number of droplets. The photograph was taken after prolonged infrared irradiation of the cluster.

librium droplet radius in the region above the boundary curve at the same temperature T_{s0} . Obviously, the value of a_{eq} increases at relatively high values of both T_{s0} and the infrared radiative flux. In further analysis, we will distinguish the “small droplets” (at the boundary curve) and “large droplets” above the boundary curve with the greater equilibrium radius.

A series of experiments showed that the droplets reach the same equilibrium radius not only in the case of small clusters, but also during infrared heating of clusters consisting of several dozen droplets. Moreover, the effect of the number of droplets in the cluster on this process is insignificant. It is only important that the distance between the relatively small equilibrium droplets of water turns out to be significantly larger than the size of the droplets themselves. An example of such a relatively large cluster at the final stage of its infrared heating is shown in Fig. 5. It is seen that the droplets in the central zone of the cluster are almost identical. The relatively small size of some droplets at the periphery of the cluster is partly due to the limited diameter of the almost isothermal spot of heating the surface of water layer, as well as to the fact that the peripheral droplets only recently joined the cluster and did not manage to reach the equilibrium.

4. Absorption of infrared radiation by water droplets

Strictly speaking, the radiation absorption by single droplets depends on the neighboring droplets and the closely spaced surface of water layer. In the cluster under consideration, the droplets are larger than the radiation wavelength and they are relatively far from each other. Therefore, the hypothesis of independent scattering is acceptable to calculate the absorption of infrared radiation by single water droplets [10–13]. The far-field effects due to the regular position of the droplets are not important in the problem under consideration. The effect of water layer is also negligible because of a small reflectance in the near-infrared spectral range. As a result, the absorption of infrared radiation by spherical droplets in the cluster can be calculated using the classical Mie theory [14–18]. Most likely, the hypothesis of independent scattering of infrared radiation by single water droplets is not true in the case of clusters containing closely spaced droplets with sizes comparable with the wavelength. However, only the clusters like that shown in Fig. 2 are considered in the present paper.

The Mie solution can be used to calculate the radiation field inside a homogeneous spherical particle at arbitrary external ir-

radiation [18–21]. In the problem under consideration, we should take into account the spectrum of the emitters of infrared radiation and integrate the absorbed radiation power over the spectrum as it was done in paper [6]. The additional calculations for one infrared emitter and water droplets with two different radii are presented in Fig. 6. The spectral optical constants of water reported in [22,23] were used in the calculations. The normalized values of absorbed power, \bar{P} (in conventional units), are plotted in this Fig. 6. The field of the absorbed radiation power is more uniform when the droplets are irradiated by two infrared emitters with the angle $\pi/2$ between their axes (as shown in Fig. 1). The incident radiation is nonuniformly absorbed in the volume of semi-transparent water droplets. As predicted by the Mie theory, the number of partial waves which contribute to the internal radiation field is determined by the diffraction parameter of the droplet, $x = 2\pi a/\lambda$. Therefore, the spatial variation of the absorbed radiation in the droplet of radius $a = 20\mu\text{m}$ is much more complex than that for the droplet with $a = 10\mu\text{m}$ [18]. However, this cannot affect the temperature field in the droplets because of heat transfer by conduction and convection. The non-uniform distribution of evaporation and condensation over the droplet surface seems to be even more important. Note that the measurements of surface temperature of water droplets in a cluster without infrared heating [24] in the range of $30 < a < 60\mu\text{m}$ can be extrapolated to the smaller values of droplet radius. The resulting difference between the minimum temperature at the top and the higher “equator” temperature of the droplet of radius $a = 20\mu\text{m}$ is about 3 °C. Obviously, this temperature difference is much less in the case of infrared heating.

Thus, the following hierarchy of spatial scales inherent for the droplet cluster under infrared irradiation emerges: $b \gg a \gg \lambda \gg l$, where b is the radius of the cluster and $l \sim 0.2\mu\text{m}$ is the mean free path of water vapor molecules at the atmospheric pressure.

Consider also that the characteristic time scale, τ_{rel} , of the thermal equilibration is “short” even for relatively large droplets. Indeed, this time scale may be roughly estimated from the equation $Fo = \alpha \tau_{rel}/a^2 = 1$, where $\alpha = k_w/(\rho_w c_w)$ is the thermal diffusivity of water and Fo is the Fourier number. Substituting $\alpha = 1.5 \cdot 10^{-7} \text{m}^2/\text{s}$ and $a = 50\mu\text{m}$ yields $\tau = 17\text{ms}$, which is much smaller than the characteristic time scales of thermal processes addressed in the paper. The hierarchy of time scales in the problem under consideration can be presented as follows: $\tau_{eq} \gg \tau_{th} \gg \tau_{rel} \gg \tau_{mol}$, where τ_{eq} is the time to reach the equilibrium droplet radius, τ_{th} is the time to reach the equilibrium droplet temperature, and τ_{mol} is the mean time of the free path of water molecules.

It the case of small isothermal droplets, it is sufficient to estimate a contribution of infrared radiation to the thermal balance of a droplet using the average efficiency factor of absorption:

$$\bar{Q}_a(a) = \int_{\lambda_1}^{\lambda_2} Q_a(\lambda, a) q_\lambda d\lambda / \int_{\lambda_1}^{\lambda_2} q_\lambda d\lambda \quad (1)$$

where Q_a is the spectral efficiency factor of absorption of a uniform spherical particle introduced in the Mie theory and q_λ is the incident spectral radiative flux. The spectrum of the infrared emitters is similar to that of the blackbody spectrum at temperature 1223 K, and this determines a choice of λ_1 and λ_2 in the calculations. The Planck function for the blackbody radiation was used instead of q_λ in the calculations based on Eq. (1). The calculated monotonic increase in \bar{Q}_a with the droplet radius (Fig. 7) is explained by increasing the optical thickness of semi-transparent water droplets [18]. The resulting increase in contribution of infrared radiation to the heat balance of a water droplet with increasing the droplet size should be taken into account in the heat transfer model.

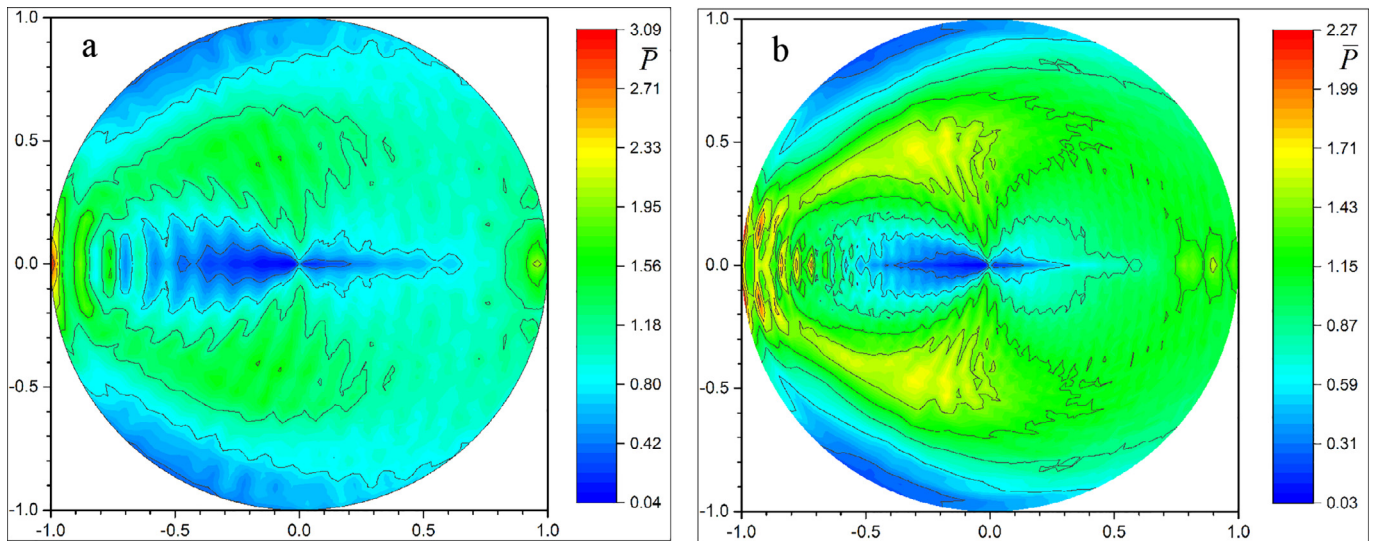


Fig. 6. The field of normalized absorbed radiation power in water droplets: a - $a = 10\mu\text{m}$, b - $a = 20\mu\text{m}$. The collimated infrared radiation illuminates the droplets on the left, along the horizontal axis. The dimensionless coordinates are normalized to the droplet radius.

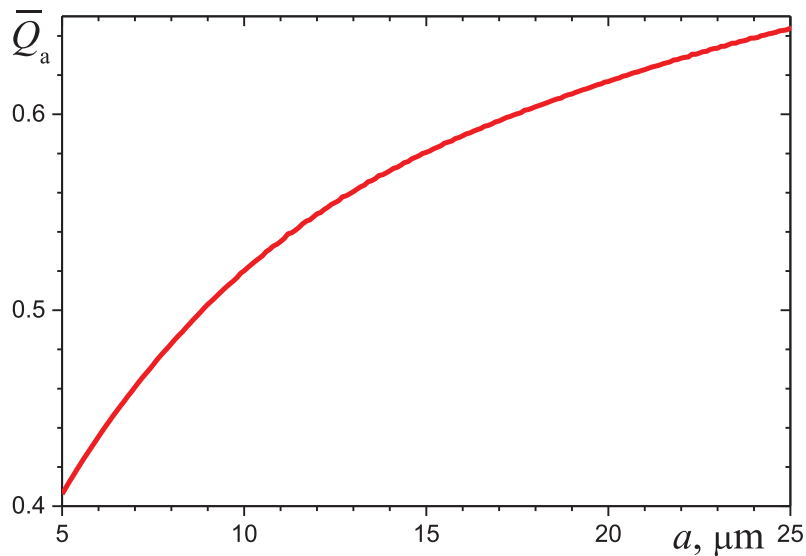


Fig. 7. The spectrally averaged efficiency factor of absorption for irradiated droplets of water.

5. Theoretical and computational analysis of heat transfer

A theoretical model for estimating the equilibrium radius of water droplets in a cluster should take into account the interaction of all thermal processes, including evaporation and condensation at the droplet surface, as well as convective heat transfer with an ascending flow of a mixture of water vapor and ambient air. It should be recalled that not only the absorption of the incident infrared radiation, but also the other components of the heat balance depend on the droplet size. Note that a similar effect of thermal radiation on size of water droplets takes place in the atmosphere and in diverse engineering problems [25–30]. At the same time, there is an important difference between water droplets in atmospheric mists or clouds and water droplets in the specific levitating cluster considered in the present study. The droplet cluster is a self-arranged regular structure of droplets levitating in a plane parallel to the substrate layer of water. From the radiation point of view, there is no multiple scattering of radiation (visible or infrared) in the cluster and the diffuse radiation field is not formed in the droplet cluster (in contrast to the natural mist and clouds). The droplets of the

levitating cluster are formed and supported by evaporation of the water layer under the cluster. In other words, the locally heated water layer and the droplet cluster form a single system in which the parameters and behavior of water droplets are determined by the features of heating and evaporation of the water layer. Obviously, the effect of external infrared heating of a droplet cluster is quite another physical problem that those considered in studies of atmospheric mists or clouds.

5.1. Transient heat transfer model for single water droplets

It is assumed that time variation of both the size and temperature of a single droplet in the so-called “small cluster” [31–33] can be considered independently of the presence of neighboring droplets. In other words, the droplets do not affect the parameters of each other, and the parameters of these droplets in the case of an external infrared irradiation can be calculated without account for the effect of other droplets in the cluster. The same value of the equilibrium radius obtained for the central droplet and peripheral droplets (see Fig. 2) can be treated as an indirect con-

firmation of a weak thermal interaction between the neighboring droplets. It goes without saying that any heat transfer model for single droplets cannot be applied to the recently studied chain-like clusters [34].

In the present paper, we consider the cluster composed of “thermally” small droplets. This enables us to neglect the temperature difference in the droplet and assume that the droplets are almost isothermal. The parameters of a single spherical water droplet with initial values of radius a_0 and temperature T_0 under the infrared irradiation are determined by the following equations:

$$\rho_w c_w \frac{dT}{dt} = \frac{3}{a} \left(\frac{\bar{Q}_a q}{4} + \dot{m}L - k_{\text{gas}} \frac{T - T_{\text{gas}}}{a} \right) \quad T(0) = T_0 \quad (2)$$

$$\rho_w \frac{da}{dt} = \dot{m} \quad a(0) = a_0 \quad (3)$$

where ρ_w and c_w are the density and specific heat capacity of water, q is the integral (over the spectrum) infrared radiative flux to the droplet from two infrared emitters (the value of q was determined using the specification of infrared emitters), \dot{m} is the resulting mass flow rate of water vapor toward the droplet due to condensation and evaporation, L is the latent heat of water evaporation/condensation, k_{gas} is the thermal conductivity of ambient gas mixture (humid air), T_{gas} is the gas temperature outside the thermal boundary layer. The coefficient in the last (convective) term of Eq. (2) is written for the Stokes flow regime characterized by the Nusselt number $\text{Nu} = 2ah/k_{\text{gas}} = 2$, where h is the convective heat transfer coefficient.

It was shown in the early papers [35–37] that first order phase transitions such as condensation of water vapor are accompanied by characteristic infrared radiation. This phenomenon, sometimes called the PeTa effect (this abbreviation means Perel'man-Tatarchenko's effect), is really important for remote sensing of the cloudy atmosphere [38–40]. However, according to [37,40], the radiative heat losses in the infrared wavelength range of $4 < \lambda < 8 \mu\text{m}$ during the condensation of water vapor do not exceed 3–5% of the latent energy of the phase transition. Therefore, the PeTa effect is neglected in the heat balance equation.

The Cauchy problem (2)–(3) for the coupled ordinary differential equations was solved numerically using the classical Runge-Kutta iterative method (RK4) and the corresponding standard computer code. It should be noted that Eq. (2) has features typical of the transient energy equation, which describes the thermal state of an evaporating or condensing small particle or thin film, characterized by low heat capacity. A very large value of the latent heat of evaporation leads to the fact that at the beginning of the process the corresponding term of the energy equation dominates and the role of the remaining terms on the right side of the equation is insignificant. This leads to a fast variation in temperature during the initial period when the droplet size or film thickness changes only slightly.

As will be shown below, in the problem under consideration, this means a fast transition to the equilibrium temperature of the droplet. It is interesting to recall the known effect when the formation of self-assembled patterns on the surface of a drying polymer film (the so-called “breath figures”) is explained by a fast evaporative cooling of the film to the dew point and subsequent condensation of small water droplets from the surrounding humid air [41–43].

The coupled Eqs. (2) and (3) should be completed by a model for water evaporation and condensation. The physical model cannot be based on the diffusion approach only and should take into account the kinetic processes in the so-called Knudsen layer at the droplet surface. This has been discussed in the early monograph by Fuchs [44] and was confirmed later by numerous experimental

studies. The mass flow rate of water vapor is determined by the following equation, which is true at arbitrary relative humidity of ambient air [45–47]:

$$\dot{m} = \frac{D p_{\text{gas}}}{a R_{\text{gas}}(T_{\text{gas}}, \varphi_{\text{gas}}) T_{\text{gas}}} \ln \frac{1 - \psi(T, \varphi_K) \varphi_K}{1 - \psi(T_{\text{gas}}, \varphi_{\text{gas}}) \varphi_{\text{gas}}} \quad (4)$$

$$\psi(T, \varphi) = \frac{p_{\text{sat}}(T)}{p_{\text{gas}}} \frac{M_{\text{vapor}}}{M_{\text{gas}}(T, \varphi)}$$

where D is the diffusion coefficient for water vapor in air, R_{gas} is the gas constant for the humid air, p_{gas} is the gas pressure, p_{sat} is the pressure of saturated water vapor, M_{vapor} and M_{gas} are the molecular masses of water vapor and humid air, φ_K and φ_{gas} are the values of relative humidity of air at the boundary of Knudsen layer and outside the boundary layer of viscous gas flow, respectively. The relative humidity at the Knudsen layer boundary is determined from the mass balance equation:

$$f_{\text{ev}} \frac{p_{\text{sat}}(T)}{\sqrt{2\pi R_{\text{vapor}} T}} (\varphi_K - 1) = \frac{D p_{\text{gas}}}{a R_{\text{gas}}(T_{\text{gas}}, \varphi_{\text{gas}}) T_{\text{gas}}} \ln \frac{1 - \psi(T, \varphi_K) \varphi_K}{1 - \psi(T_{\text{gas}}, \varphi_{\text{gas}}) \varphi_{\text{gas}}} \quad (5)$$

This equation was used to determine the value of φ_K . This was done at every time step of the iterative computational procedure. The known equations for the molecular mass and gas constant of humid air are:

$$M_{\text{gas}}(T, \varphi) = \frac{R}{R_{\text{gas}}(T, \varphi)} \quad R_{\text{gas}}(T, \varphi) = R_{\text{air}} \left(1 - \varphi \left(1 - \frac{M_{\text{vapor}}}{M_{\text{air}}} \right) \frac{p_{\text{sat}}(T)}{p_{\text{gas}}} \right) \quad (6)$$

where $R = 8314 \text{ J}/(\text{kmol K})$ is the universal gas constant. The pressure of the saturated vapor of water is calculated using the Antoine equation with the parameters determined on the basis of early data reported by Stull [48], as it was done in paper [29]:

$$\lg p_{\text{sat}}(T) = 4.6543 - \frac{1435.264}{T - 64.848} \quad (7)$$

where T is measured in Kelvin and p_{sat} is obtained in bar (10^5 Pa). The dimensionless coefficient f_{ev} in Eq. (5) was introduced in papers [47,49] to avoid very time-consuming numerical solution for the coupled Boltzmann kinetic equations. Strictly speaking, the coefficient f_{ev} is a function of the condensation coefficient, the ratio of partial pressures of water vapor and air, and the temperatures of the interface and ambient medium. However, one can use the constant value of $f_{\text{ev}} = 0.0024$ for water droplets in air [49]. Note that the above model has been validated by comparison with experimental data of [50] for evaporation of water droplets in ambient air. The model with the above constant value of f_{ev} is expected to be a reasonable approach in the range of the main parameters of the problem under consideration.

5.2. The equilibrium conditions for small droplets

Obviously, the above formulated problem has an asymptotic solution at $t \rightarrow \infty$ corresponding to the equilibrium values of both the radius and temperature of water droplet. The equilibrium conditions are $\dot{m} = 0$ and $\dot{T} = 0$. The resulting energy balance for the equilibrium droplet with radius a_{eq} and temperature T_{eq} is as follows:

$$0.75 \bar{Q}_a q = 3 k_{\text{gas}} (T_{\text{eq}} - T_{\text{gas}}) / a_{\text{eq}} \quad (8)$$

In further analysis, we assume that T_{gas} is equal to the measured surface temperature of water layer, T_s . This assumption seems to be realistic because the height of the cluster levitation

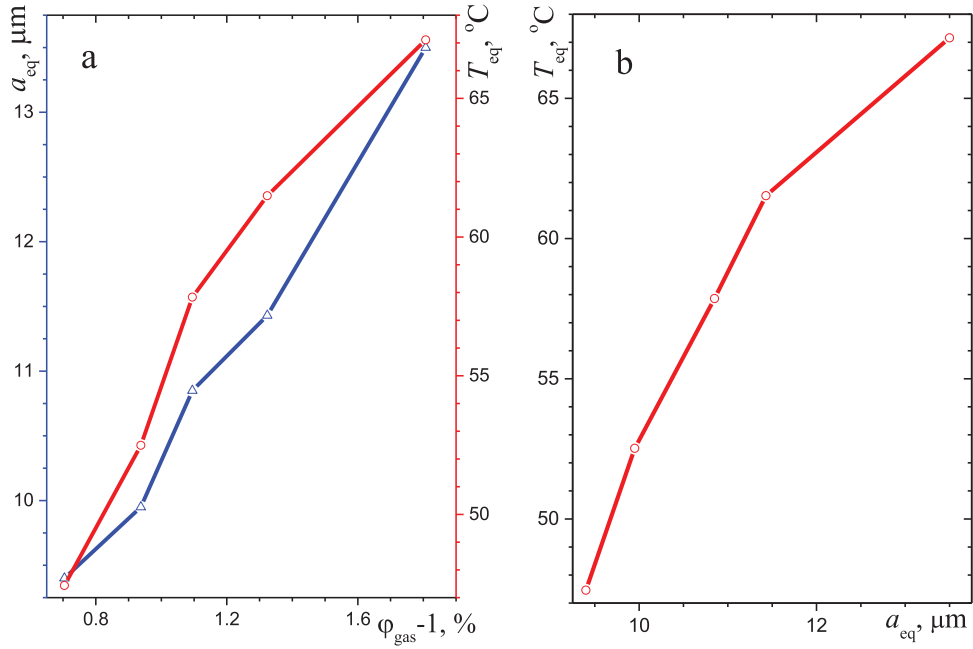


Fig. 8. Parameters of equilibrium water droplets: (a) effect of humidity of ambient air on droplet radius and temperature, (b) dependence of equilibrium droplet temperature on droplet radius.

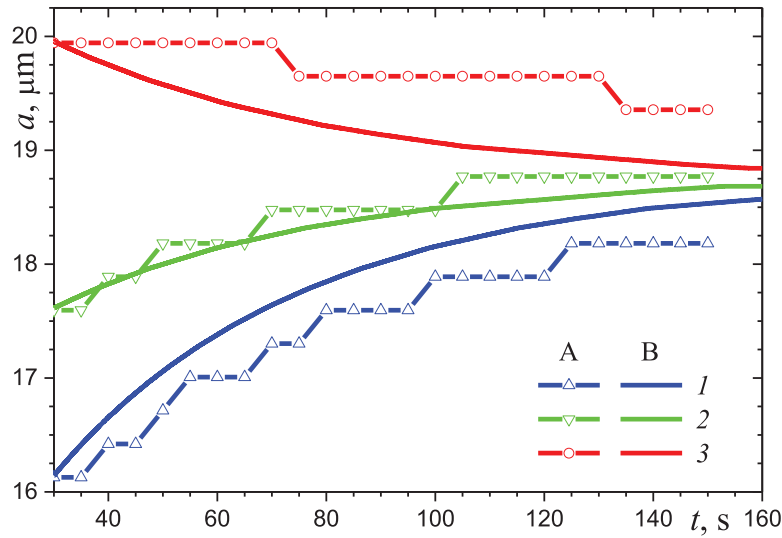


Fig. 9. Time variation of droplet radius during the infrared heating: comparison of (A) experimental data and (B) numerical calculations: 1, 2, and 3 are the variants with different initial radii of water droplets.

is comparable with the droplet size [51]. In this case, Eq. (8) is sufficient to obtain the value of T_{eq} for every value of a_{eq} :

$$T_{eq} = T_s + \frac{a_{eq}}{4k_{gas}} \bar{Q}_a q \quad (9)$$

According to Eqs. (4) and (5), the conditions of mass balance at the droplet surface are:

$$\psi(T_{eq}, \varphi_K) \varphi_K = \psi(T_s, \varphi_{gas}) \varphi_{gas} \quad \varphi_K = 1 \quad (10)$$

After simple transformations, one can obtain the following simple equation for φ_{gas} :

$$\varphi_{gas} = p_{sat}(T_{eq})/p_{sat}(T_s) \quad (11)$$

Let us consider several variants of experimentally observed equilibrium droplets. These variants are specified in Table 1.

The following values of physical parameters are used in subsequent calculations: $D = 2.6 \cdot 10^{-5} \text{m}^2/\text{s}$, $R_{vap} = 461.7 \text{J}/(\text{kg K})$,

Table 1

The experimental parameters for the minimum radii of equilibrium water droplets.

$T_s, ^{\circ}\text{C}$	47.3	52.3	57.6	61.2	66.7
$q, \text{mW}/\text{mm}^2$	3.01	3.85	4.19	4.86	5.58
$a_{eq}, \mu\text{m}$	9.4	9.95	10.85	11.4	13.5

$R_{air} = 286.5 \text{J}/(\text{kg K})$, $p_{gas} = 0.1 \text{MPa}$, $k_{gas} = 0.026 \text{W}/(\text{m K})$, $\rho_w = 10^3 \text{kg}/\text{m}^3$, $c_w = 4.18 \text{kJ}/(\text{kg K})$, and $L = 2.26 \text{MJ}/\text{kg}$. For the simplicity, the insignificant effect of temperature on the above thermal properties is not considered in the approximate numerical calculations. The results of calculations with the use of Eqs. (9) and (11) are presented in Fig. 8. As one can expect, both the radius and temperature of equilibrium droplets are almost directly proportional to the oversaturation of water vapor in ambient humid

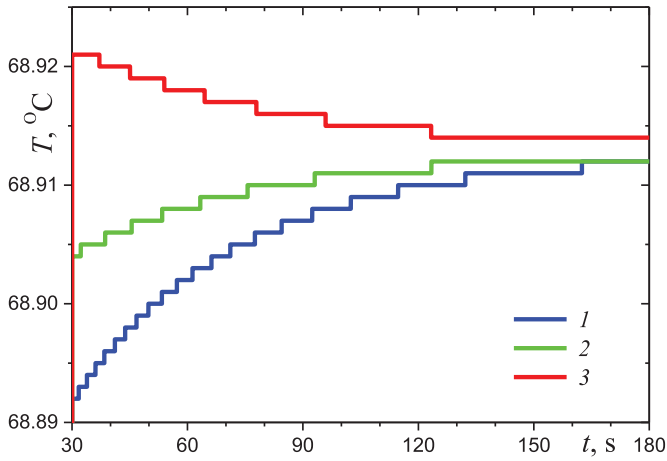


Fig. 10. Calculated time variation of temperature of water droplets: 1, 2, and 3 are the variants with different initial radii of water droplets.

air (Fig. 8a). According to Eq. (9), the monotonic increase in T_{eq} with a_{eq} is also observed (Fig. 8b). This is explained by a contribution of both terms in the right-hand side of Eq. (9) because the increase in a_{eq} is related with the increase in T_s (see Table 1). Note that the equilibrium temperature of the droplets is only slightly higher than the surface temperature of the lower layer of water. This is also quite clear from Eq. (9) because of very small value of the equilibrium radius of the droplets.

It should be noted that the local oversaturation of water vapor in the gas flow is typical for droplet clusters. Indeed, just this oversaturation is the only physical reason for the droplet growth in the case when there is no external infrared heating [5].

5.3. Numerical analysis of a transition to the equilibrium

The time dependences of radius calculated for larger droplets using the theoretical model (2)–(5) and the known function of $\dot{Q}_a(a)$ are presented in Fig. 9. The calculations were performed

for three variants of experimental conditions corresponding to the droplets with numbers 2, 4, and 5 in Figs. 2 and 3 (the numbers of these variants are 1, 2, and 3, respectively). The time interval of $0 < t < 30$ s was not considered because of variable experimental conditions during this period. The further process was characterized by the constant values of both $T_s = 69.3$ °C and $q = 5.58$ mW/mm² for all the variants.

The predicted equilibrium parameters of the droplets under consideration are $a_{eq} \approx 18.8$ μm and $T_{eq} = 68.9$ °C ($\varphi_{gas,eq} \approx 1.03$). The initial temperature of the droplets (at $t = 30$ s) does not affect the calculated dependences of $a(t)$ because the equilibrium temperature is reached very fast (see Fig. 10). As discussed above, such a result is typical for the problems of evaporation and condensation due the very high latent heat of the phase change.

The discrepancy between the computational and experimental results for the droplet radius (Fig. 9) is explained by the assumption of the same equilibrium humidity of ambient air during the process for different droplets. Obviously, this assumption is acceptable for variant 2 only when the initial radius of water droplet of $a_0 = 17.6$ μm (at $t = 30$ s), which is close to the equilibrium value of the droplet radius. On the contrary, water droplets with $a_0 = 16.1$ μm and 19.9 μm (variants 1 and 3) are characterized by considerable condensation and evaporation, respectively. This means that the relative humidity of ambient air used in the calculations should be corrected.

It is interesting to look at the calculated dependences of $T_{eq}(a_{eq})$ and $\varphi_{gas,eq}(a_{eq})$ for the conditions of the experiment under consideration: $T_s = 69.3$ °C and $q = 5.58$ mW/mm². These dependences presented in Fig. 11 are almost linear and can be simply approximated. The equilibrium temperature of water droplets increases slightly with the droplet radius (Fig. 11a), and this minor effect is not important for the computational modeling. On the contrary, the increase in the humidity of ambient air leads to a considerable increase in the equilibrium droplet radius. The computational data for the relative humidity presented in Fig. 11b can be approximated as follows:

$$\varphi_{gas,eq}(a_{eq}) = 1 + 0.01 \left(1.7 \frac{a_{eq}}{a_1} - 0.5 \right) \quad a_1 < a_{eq} < 2a_1 \quad (12)$$

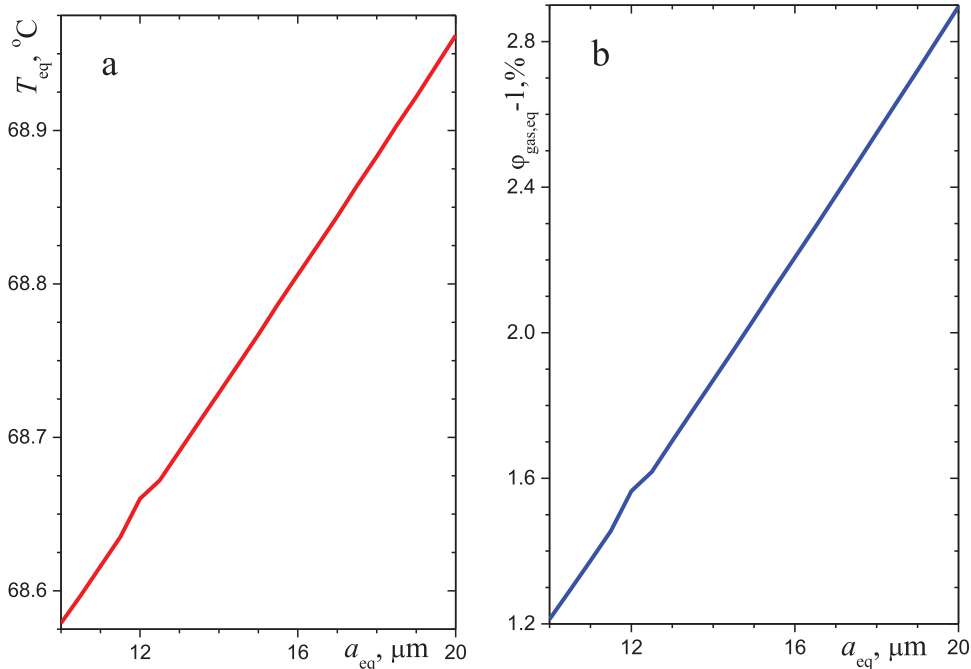


Fig. 11. Effect of radius of equilibrium water droplets on (a) the droplet temperature and (b) the humidity of ambient air.

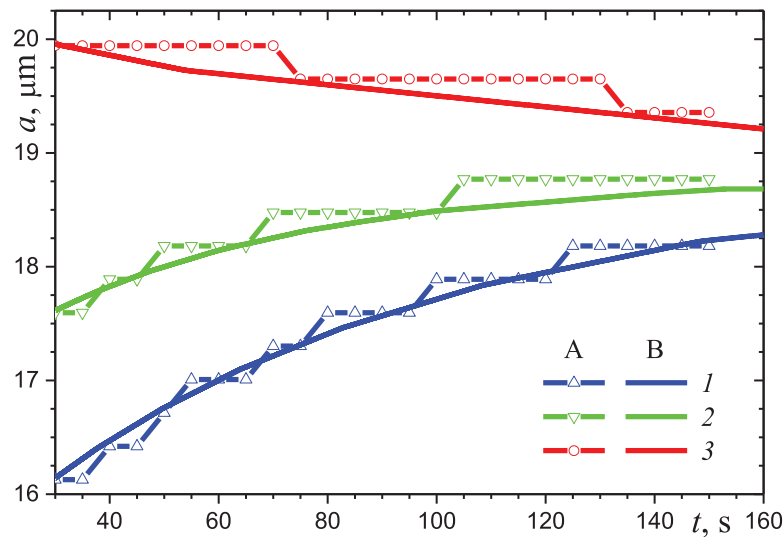


Fig. 12. Time variation of droplet radius during the infrared heating: comparison of (A) experimental data and (B) numerical prediction based on the corrected model: 1, 2, and 3 are the variants with different initial radii of water droplets.

where $a_1 = 10\mu\text{m}$.

Of course, at constant atmospheric pressure, the current relative humidity of air surrounding the water droplets is determined mainly by the surface temperature of water layer under the cluster. At the same time, the predominant evaporation and condensation of non-equilibrium droplets affect the value of φ_{gas} outside the thermal boundary around the droplet. It is natural to assume that the relative humidity of air surrounding non-equilibrium droplets during their predominant evaporation or the condensational growth is intermediate between the quasi-steady value for the current droplet size and the limiting value reached for the equilibrium droplet. This can be written as follows:

$$\varphi_{\text{gas}}(t) = \gamma \varphi_{\text{gas,eq}}(a_{\text{eq}}) + (1 - \gamma) \varphi_{\text{gas,eq}}(a) \quad (13)$$

Obviously, one can use the value of $\gamma = 1$ when the initial value of droplet radius is close to the equilibrium value, whereas $\gamma < 1$ is a better choice in the case of a significant difference between the initial and final radii of the droplet. A comparison of the corrected computational model (according to Eq. (13)) and the experimental data for the radii of water droplets is presented in Fig. 12. No correction was used in calculations for variant 2 ($\gamma = 1$), and the values of $\gamma = 0.4$ and $\gamma = 0.6$ were chosen for variants 1 and 3. The numerical results indicate that the suggested correction of the current relative humidity of ambient air enabled us to get good accuracy of the computational predictions during the entire process. This confirms an important role of humidity of ambient air in the process of reducing or increasing the size of water droplets in the cluster.

6. Conclusions

The asymptotic behavior of the levitating droplet cluster stabilized by a long-term infrared irradiation was experimentally studied for the first time. The monotonic decrease in the equilibrium size of water droplets with the intensity of incident radiation was obtained.

The developed theoretical model for transient heat transfer takes into account the thermal effect of infrared radiation, the dynamics of evaporation and condensation, as well as convective heat transfer with the surrounding humid air. Simple analytical relations are obtained for the asymptotic equilibrium parameters of small droplets.

The numerical data for the time variation in the radius of small cluster droplets in the ascending flow of a mixture of air and water vapor are in good agreement with the results of laboratory measurements. The problem analysis confirms the important role of the local overheating of the lower layer of water on the degree of oversaturation of water vapor and the resulting parameters of the droplet cluster.

Declaration of Competing Interest

None declared.

Acknowledgements

The authors gratefully acknowledge the Russian Science Foundation (project 19-19-00076) for the financial support of this work. V.Yu. Levashov's work was carried out within the framework of the scientific plan of the Institute of Mechanics of Moscow State University (No. AAAA-A19-119012990112-4).

References

- [1] A.A. Fedorets, Droplet cluster, *JETP Lett.* 79 (8) (2004) 372–374.
- [2] E.A. Arinstein, A.A. Fedorets, Mechanism of energy dissipation in a droplet cluster, *JETP Lett.* 92 (10) (2010) 658–661.
- [3] A.A. Fedorets, I.V. Marchuk, O.A. Kabov, On the role of capillary waves in the mechanism of coalescence of a droplet cluster, *JETP Lett.* 99 (5) (2014) 266–269.
- [4] A.A. Fedorets, M. Frenkel, E. Shulzinger, L.A. Dombrovsky, E. Bormashenko, M. Nosonovsky, Self-assembled levitating clusters of water droplets: pattern-formation and stability, *Sci. Rep.* 7 (2017) 1888.
- [5] A.A. Fedorets, L.A. Dombrovsky, D.N. Medvedev, Effect of infrared irradiation on the suppression of the condensation growth of water droplets in a levitating droplet cluster, *JETP Lett.* 102 (7) (2015) 452–454.
- [6] L.A. Dombrovsky, A.A. Fedorets, D.N. Medvedev, The use of infrared irradiation to stabilize levitating clusters of water droplets, *Infrared Phys. Techn.* 75 (2016) 124–132.
- [7] A.A. Fedorets, L.A. Dombrovsky, Generation of levitating droplet clusters above the locally heated water surface: a thermal analysis of modified installation, *Int. J. Heat Mass Transfer* 104 (2017) 1268–1274.
- [8] A.A. Fedorets, L.A. Dombrovsky, Self-assembled stable clusters of droplets over the locally heated water surface: milestones of the laboratory study and potential biochemical applications, in: *Proc. 16th Int. Heat Transfer Conf.*, Aug. 10–15, Beijing, China, 2018 Keynote lecture IHTC16-KN02.
- [9] A.A. Fedorets, E. Bormashenko, L.A. Dombrovsky, M. Nosonovsky, Droplet clusters: nature-inspired biological reactors and aerosols, *Philos. Trans. Royal Soc. A* 377 (2019) 20190121.
- [10] C.L. Tien, B.L. Drolen, Thermal radiation in particulate media with dependent and independent scattering, in: *Annual Review of Numerical Fluid Mechanics and Heat Transfer*, 1, Hemisphere, New York, 1987, pp. 1–32.

- [11] A.A. Kokhanovsky, *Optics of Light Scattering Media: Problems and Solutions*, 3rd Ed., Praxis, Chichester, UK, 2004.
- [12] M.I. Mishchenko, *Electromagnetic Scattering by Particles and Particle Groups: An Introduction*, Cambridge University Press, CambridgeUK, 2014.
- [13] M.I. Mishchenko, "Independent" and "dependent" scattering by particles in a multi-particle group, *OSA Continuum* 1 (1) (2018) 243–260.
- [14] H.C. van de Hulst, *Light Scattering by Small Particles*, Wiley, New York, 1957 (also Dover Publ., New York, 1981).
- [15] C.F. Bohren, D.R. Huffman, *Absorption and Scattering of Light by Small Particles*, Wiley, New York, 1983.
- [16] L.A. Dombrovsky, *Radiation Heat Transfer in Disperse Systems*, Begell House, New York, 1996.
- [17] M.I. Mishchenko, L.D. Travis, A.A. Lacis, *Scattering, Absorption, and Emission of Light by Small Particles*, Cambridge Univ. Press, Cambridge, 2002.
- [18] L.A. Dombrovsky, D. Baillis, *Thermal Radiation in Disperse Systems: An Engineering Approach*, Begell House, New York, 2010.
- [19] A. Tuntomo, C.L. Tien, S.H. Park, Internal distribution of radiant absorption in a spherical particle, *ASME J. Heat Transf.* 113 (2) (1991) 407–412.
- [20] P.L.C. Lage, R.H. Rangel, Total thermal radiation absorption by a single spherical droplet, *J. Thermophys. Heat Transf.* 7 (1) (1993) 101–109.
- [21] L.A. Dombrovsky, Thermal radiation from nonisothermal spherical particles of a semitransparent material, *Int. J. Heat Mass Transf.* 43 (9) (2000) 1661–1672.
- [22] G.M. Hale, M.P. Querry, Optical constants of water in the 200 nm to 200 μm wavelength region, *Appl. Optics* 12 (3) (1973) 555–563.
- [23] V.M. Zolotarev, A.V. Dyomin, Optical constants of water in wide wavelength range 0.1 \AA –1 m, *Optics Spectr.* 43 (1977) 271–279.
- [24] A.A. Fedorets, L.A. Dombrovsky, A.M. Smirnov, The use of infrared self-emission measurements to retrieve surface temperature of levitating water droplets, *Infrared Phys. Techn.* 69 (2015) 238–243.
- [25] C.C. Tseng, R. Viskanta, Enhancement of water droplet evaporation by radiation absorption, *Fire Safety J.* 41 (3) (2006) 236–247.
- [26] G. Miliauskas, V. Sabanas, Interaction of transfer processes during unsteady evaporation of water droplets, *Int. J. Heat Mass Transf.* 49 (11–12) (2006) 1790–1803.
- [27] M.Q. Brewster, Evaporation and condensation of water mist/cloud droplets with thermal radiation, *Int. J. Heat Mass Transf.* 88 (2015) 695–712.
- [28] M.Q. Brewster, Corrigendum to "Evaporation and condensation of water mist/cloud droplets with thermal radiation", *Int. J. Heat Mass Transf.* 88 (2015) 695–712 *Int. J. Heat Mass Transf.* 96 (2016) 703–704.
- [29] L.A. Dombrovsky, S. Dembele, J.X. Wen, An infrared scattering by evaporating droplets at the initial stage of a pool fire suppression by water sprays, *Infrared Phys. Techn.* 91 (2018) 55–62.
- [30] L.A. Dombrovsky, V.Yu. Levashov, A.P. Kryukov, S. Dembele, J.X. Wen, A comparative analysis of shielding of thermal radiation of fires using mist curtains containing droplets of pure water or sea water, *Int. J. Thermal Sci.* 152 (2020) 106299.
- [31] A.A. Fedorets, M. Frenkel, E. Bormashenko, M. Nosonovsky, Small levitating ordered droplet clusters: stability, symmetry and Voronoi entropy, *J. Phys. Chem. Lett.* 8 (22) (2017) 5599–5602.
- [32] E. Bormashenko, A.A. Fedorets, M. Frenkel, L.A. Dombrovsky, L.A., M. Nosonovsky, Clustering and self-organization in small scale natural and artificial systems, *Philos. Trans. Royal Soc. A* 378 (2020) 20190443.
- [33] A.A. Fedorets, E. Bormashenko, L.A. Dombrovsky, M. Nosonovsky, Symmetry of small clusters of levitating water droplets, *Phys. Chem. Chem. Phys.* 22 (21) (2020) 12233–12244.
- [34] A.A. Fedorets, M. Frenkel, I. Legchenkova, D. Shcherbakov, L. Dombrovsky, M. Nosonovsky, E. Bormashenko E, Self-arranged levitating droplet clusters: a reversible transition from hexagonal to chain structure, *Langmuir* 35 (2019) 15330–15334.
- [35] W.R. Potter, J.G. Hoffman, Phase transition luminescence in boiling water; evidence for clusters, *Infrared Phys* 8 (1968) 265–270.
- [36] M.E. Perel'man, Phase transitions caused by the opening of new channels in electron-photon interactions, *Phys. Lett.* 37A (5) (1971) 411–412.
- [37] A.N. Mestvirishvili, J.G. Directovich, S.I. Grigoriev, M.E. Perel'man, Characteristic radiation due to the phase transitions latent energy, *Phys. Lett.* 60A (2) (1977) 143–144.
- [38] M.E. Perel'man, V.A. Tatarchenko, Phase transitions of the first kind as radiation processes, *Phys. Lett. A* 372 (14) (2008) 2480–2483.
- [39] K.-T. Wang, M.Q. Brewster, Phase-transition radiation in vapor condensation process, *Int. Commun. Heat Mass Transf.* 37 (8) (2010) 945–949.
- [40] V.A. Tatarchenko, Characteristic infrared radiation of the first-order phase transitions and its connection with atmospheric optics, *Atmos. Ocean. Opt.* 23 (4) (2010) 252–258.
- [41] A. Muñoz-Bonilla, M. Fernández-García, J. Rodríguez-Hernández, Towards hierarchically ordered functional porous polymeric surfaces prepared by the breath figures approach, *Prog. Polym. Sci.* 39 (3) (2014) 510–554.
- [42] E. Bormashenko, Breath-figure self-assembly, a versatile method of manufacturing membranes and porous structures: physical, chemical and technological aspects, *Membranes* 7 (3) (2017) 45.
- [43] L.A. Dombrovsky, M. Frenkel, I. Legchenkova, E. Bormashenko, Effect of thermal properties of a substrate on formation of self-arranged surface structures on evaporated polymer films, *Int. J. Heat Mass Transf.* 158 (2020) 120053.
- [44] N.A. Fuchs, *Evaporation and Droplet Growth in Gaseous Media*, Pergamon Press, London, 1959.
- [45] A.P. Kryukov, V.Yu. Levashov, S.S. Sazhin, Evaporation of diesel fuel droplets: kinetic versus hydrodynamic models, *Int. J. Heat Mass Transf.* 47 (12–13) (2004) 2541–2549.
- [46] A.P. Kryukov, V.Yu. Levashov, I.N. Shishkova, Evaporation in mixture of vapour and gas mixture, *Int. J. Heat Mass Transf.* 52 (23–24) (2009) 5585–5590.
- [47] V.Yu. Levashov, A.P. Kryukov, Numerical simulation of water droplet evaporation into vapor-gas medium, *Colloid J.* 79 (5) (2017) 647–653.
- [48] D.R. Stull, Vapor pressure of pure substances. Organic and inorganic compounds, *Industr. Eng. Chem.* 39 (4) (1947) 517–550.
- [49] V.Yu. Levashov, A.P. Kryukov, I.N. Shishkova, Influence of the noncondensable component on the characteristics of temperature change and the intensity of water droplet evaporation, *Int. J. Heat Mass Transf.* 127 (2018) 115–122.
- [50] V.Yu. Borodulin, V.N. Letushko, M.I. Nizovtsev, A.N. Sterlyagov, Determination of parameters of heat and mass transfer in evaporating drops, *Int. J. Heat Mass Transf.* 109 (2017) 609–618.
- [51] A.A. Fedorets, L.A. Dombrovsky, D.N. Gabyshev, E. Bormashenko, M. Nosonovsky, Effect of external electric field on dynamics of levitating water droplets, *Int. J. Therm. Sci.* 153 (2020) 106375.